Preliminary study of contrast-enhanced multidetector computed tomography scanning for the differentiation of perigastric tumor deposits from metastatic lymph nodes in gastric cancer

Wei-zhi Chen (cghcwz@163.com)
The First Affiliated Hospital of Jinzhou Medical University

Han Gao
The First Affiliated Hospital of Jinzhou Medical University

Na Xu
The First Affiliated Hospital of Jinzhou Medical University

Yu-bin Wang
The First Affiliated Hospital of Jinzhou Medical University

Cheng Li
The First Affiliated Hospital of Jinzhou Medical University

Jing Yang
The First Affiliated Hospital of Jinzhou Medical University

Xin-yue Li
The First Affiliated Hospital of Jinzhou Medical University

Research Article

Keywords: gastric cancer, tumor deposits, metastatic lymph nodes, multidetector computed tomography

Posted Date: April 18th, 2022

DOI: https://doi.org/10.21203/rs.3.rs-1544107/v1

Abstract

Purpose: To investigate the diagnostic value of contrast-enhanced multidetector computed tomography (MDCT) scanning for the differentiation of perigastric tumor deposits (TDs) from metastatic lymph nodes in gastric cancer.

Methods: In this prospective study, 36 patients with gastric cancer confirmed by surgical pathology between December 2020 and December 2021 underwent preoperative noncontrast and three-phase contrast-enhanced MDCT scans. According to the postoperative pathological results, the nodules were divided into a TD group and a metastatic lymph node (MLN) group. The observed CT imaging characteristics included lesion morphology, necrosis, long-axis diameter, short-axis diameter, aspect ratio, and corrected CT attenuation value (cCAV) in each phase. The lesion parameters of the two groups were compared, and receiver operating characteristic (ROC) curves were used to evaluate and analyze the diagnostic efficacy of MDCT.

Results: A total of 30 TDs and 55 MLNs were detected in 36 patients. Among the 30 TDs, 21 had irregular morphology, and 15 had liquefactive necrosis. In addition to necrosis and the aspect ratio, the lesion morphology, long-axis diameter, short-axis diameter, and cCAV in each phase were significantly different between the TD group and the MLN group (P<0.05). Irregular lesion morphology, long-axis diameter, short-axis diameter, and cCAV in each phase all had areas under the ROC curves (AUCs) greater than 0.685 for TD diagnosis. Among these measurements, the cCAV in the delayed phase (AUC=0.766) had the highest diagnostic efficacy. The optimal diagnostic threshold was 32.94%, the corresponding diagnostic sensitivity was 80.00%, and the specificity was 67.27%.

Conclusions: In gastric cancer, contrast-enhanced MDCT scanning is a potential technique to predict TDs and MLNs.

Introduction

Gastric cancer is a major global disease. It is the fifth most prevalent malignancy in the world, with an estimated 1 million new cases each year[1]. Accurate staging of gastric cancer is important for determining treatment options and prognosis[2, 3]. In the 8th edition of the Gastric Cancer Staging Manual, the American Joint Committee on Cancer (AJCC) proposed a staging system that includes not only (T), node (N), and metastasis (M) parameters but also registry data collection variables, including traditional histopathological features such as tumor deposits (TDs), lymphatic vascular invasion, and perineural invasion. However, the new staging system does not explain how these registry data collection variables affect tumor staging or how they can be used to guide clinical work [4].

TDs were first discovered by Gabriel in 1935 in rectal cancer [5]. Puppa et al. [6] reported that TDs are not limited to colorectal cancer but are also common in other types of cancers, including gastric cancer, bile duct cancer, and pancreatic cancer. The role and significance of TDs in colorectal cancer are widely recognized and have been discussed extensively, and attention to the role of TDs in gastric cancer has

gradually increased in recent years. In the 8th edition of the AJCC Gastric Cancer Staging Manual, TDs are defined as discontinuous tumor nodules in the lymphatic drainage area of the primary cancer, with no recognizable lymph node tissue, blood vessels, or nerve structures, and are regarded as metastatic lymph nodes (MLNs) [4]. Many studies have shown that TDs can be considered an independent risk factor for the prognosis of patients with gastric cancer and have suggested that TDs should be included in TNM staging [7, 8]. Gu et al. [9] conducted a retrospective analysis of 3098 patients with gastric cancer and found that for all patients, stage II patients and stage III patients, the 5-year disease-free survival rate was lower in the TD-positive group than in the TD-negative group (P = 0.001, 0.029 and 0.003, respectively). A study by Peparini [10] found that TDs appear to have a deleterious influence on outcomes not only in patients without lymph node involvement but also in patients with lymph node involvement. In addition, some [10, 11] have strongly recommended that TDs adjacent to gastric cancer be treated as serosa invasion requiring complete resection and adjuvant chemotherapy. Thus, the accurate identification of TDs before surgery is of great significance for the selection of appropriate treatment options and the assessment of prognosis.

Computed tomography (CT) scanning is a routine examination performed for patients with gastric cancer, and its potential for assessing tumor location and disease staging and monitoring treatment has been confirmed. However, in general CT scans, perigastric TDs in gastric cancer are often misidentified as MLNs due to an incomplete understanding of TDs. Currently, perigastric TDs in gastric cancer are mainly diagnosed based on postoperative pathology, and very few preoperative examinations are available to assess the presence of TDs. This study explored the diagnostic value of contrast-enhanced multidetector computed tomography (MDCT) scanning for perigastric TDs in gastric cancer through a prospective analysis to provide information for clinical and patient prognosis.

Materials And Methods

Patients

The hospital's Ethics Committee accepted the trial, and all patients gave written informed consent. Eighty-seven consecutive patients with gastric cancer diagnosed by gastroscopy were considered for inclusion between December 2020 and December 2021. A total of 36 patients (age range 46–92 years) were finally enrolled according to the following criteria (Fig. 1):

Inclusion criteria:

(1) The patient was histopathologically diagnosed with gastric adenocarcinoma.

(2) The patient underwent noncontrast and three-phase contrast-enhanced MDCT scans before surgery. The noncontrast CT scans and arterial, venous and delayed phase CT scans were all thin-slice scans, and all images were uploaded to a picture archiving and communication system (PACS). Additionally, the image quality met diagnostic needs.

(3) The perigastric MLNs or TDs on the CT images had a short-axis diameter greater than 5 mm to allow measurement of the CT parameters [12].

Exclusion criteria:

(1) The patient received radiotherapy or chemotherapy before surgery.

(2) The patient was allergic to the contrast material or scopolamine hydrochloride.

(3) The patient had multiple tumors with extensive metastasis to the organs, peritoneum, or omentum and did not receive surgical treatment.

(4) No lesion specimens were collected after surgery, or the collected TD and MLN specimens could not be completely matched with the CT images.

CT examination methods

All patients underwent CT examination within one week before radical gastrectomy. To ensure that the gastric cavity was fully dilated, they were required to fast for at least 8 hours before the examination, and they received an intramuscular injection of scopolamine hydrochloride (1 mL: 10 mg, Minsheng Pharmaceutical Co., Ltd., Hangzhou, China) and were required to drink 1000–1500 ml of water 10–15 min before the examination (scopolamine hydrochloride cannot be used in patients with benign prostatic hyperplasia or glaucoma). The patients were scanned in the supine position with a CT scanner (Philips Brilliance 256-slice i CT scanner, Netherlands) from the dome of the diaphragm to the umbilical level during a single breath hold. MDCT scanning was performed on all patients in the supine position using a standard algorithm and 512×512 matrix size at 120 kV and 300 mA in all cases. After noncontrast scanning (0 seconds), the examiner used an autoinjector to inject 350 mg/ml iodophor (Hengrui Pharmaceutical Co., Ltd. Jiangsu, China) into the patient's cubital vein at 3.0–5.0 ml/s; the dose was calculated by multiplying the patient's weight by 1.5 ml/kg. Arterial, venous, and delayed phase images were obtained 25–30, 65–70, and 110–120 seconds [13] after the injection of the contrast agent, respectively. All datasets were uploaded to the PACS.

Image analysis and image data acquisition

Two radiologists with 15 (N.X.) and 5 (H.G.) years of experience in abdominal imaging diagnosis performed the analysis without knowing the pathological results of perigastric TDs in patients diagnosed with gastric cancer. In the event of disagreement, consensus was achieved in consultation with a senior radiologist with 30 years of experience in abdominal radiology. All measurable nodules (short diameter > 5 mm) were marked as target nodules on the original image to prevent confusion between the image and the surgical results. The evaluation included observation and measurement of the morphology (circle and oval shapes were defined as regular shapes, while nodules with burrs and lobular changes were defined as irregular shapes), size, and enhancement characteristics (nodules with circular enhancement and no enhancement in the necrotic area were defined as necrosis) of the TDs or MLNs. The window level (WL) and window width (WW) were set to 60 and 360, respectively. The regions of interest (ROIs) were

manually delineated. Vessel structures, ulceration, necrosis, and artifacts were avoided in the ROIs, and the noncontrast and three-phase contrast-enhanced CT values of the TDs or MLNs were measured and recorded. Then, the PACS automatically read the CT values of all pixels within the ROI and calculated the average CT attenuation value (CAV). In addition, to eliminate patient-related confounding factors such as differences in contrast agent and individual absorption capacity, the two radiologists also measured the CAV on the same slice of the aortic canal to calculate the corrected CT attenuation value (cCAV). The cCAV was calculated using the following equations: (CAV of the ROI in the noncontrast phase)/(CAV in the aortic canal in the noncontrast phase) and [(CAV of the ROI in each contrast-enhanced phase)−(CAV of the ROI in the noncontrast phase)]/(CAV in the aortic canal in the corresponding contrast-enhanced phase).

Matching of TDs and MLNs on CT images with postoperative specimens

The TDs and MLNs on the CT images were matched in one-to-one correspondence with postoperative specimens through preoperative image positioning, intraoperative nodule tracking, and postoperative pathological identification. Before surgery, the radiologists and surgeons reviewed the CT images together and recorded the positions and sizes of the nodules in relation to anatomical structures such as adjacent organs (gastric cardia, gastric pylorus, greater curvature, lesser curvature, etc.) and blood vessels (e.g., common hepatic artery, left gastric artery, and splenic artery). The surgeon could thus accurately identify these nodules during the surgery, dissect them separately from the gastric tumor, and send them in separate packaging to the pathology department.

Postoperative pathological findings

All resected specimens were fixed in 10% formalin, embedded in paraffin, and stained with hematoxylin and eosin. The gastric specimens that contained cancer foci and the nodules sent for pathology examination were cut into 3-μm-thick sections, and the maximum invasion depth of the tumors or nodules or the presence of cancer cells was determined independently by two pathologists. Discrepancies in diagnosis were resolved by discussion. TD positivity was evaluated by referring to the 8th edition of the AJCC Gastric Cancer Staging Manual [4], which defines isolated tumor nodules without residual lymphoid structures, blood vessels, or nerve tissues as TD-positive nodules (Fig. 2).

Analytical content

All patients underwent radical gastrectomy and LN and TD dissection. Clear pathology reports included the tumor stage, number of MLNs, and number of TDs. The analytical content mainly comprised a comparison of the imaging morphology (regular/irregular) and sizes of TDs and MLNs and a comparison of the cCAV in each phase of the TDs and MLNs.

Statistical analysis

Statistical analysis was performed using SPSS 17.0. The intraclass correlation coefficient (ICC) was used to analyze the consistency of the parameter measurements between the two radiologists. An ICC value ≤

0.2 indicated poor consistency, 0.21–0.40 indicated fair consistency, 0.41–0.60 indicated moderate consistency, 0.61–0.80 indicated good consistency, and ≥ 0.81 indicated excellent consistency. Nonnormally distributed continuous data are expressed as medians (interquartile ranges), and categorical variables are expressed as frequencies and percentages. The Mann–Whitney U test was used to compare the differences in quantitative CT parameters, such as the lesion size and cCAV in each phase, between the TD group and the MLN group. Categorical variables were analyzed using the chi-square test. The optimal threshold for the diagnosis of TDs was determined using the sensitivity and specificity of the receiver operating characteristic (ROC) curve and the area under the ROC curve (AUC). $P < 0.05$ was considered statistically significant.

Results

A total of 36 gastric cancer patients (10 females and 26 males aged 46–92 years) were enrolled, including three (8.3%) T1/2 patients, eight (22.2%) T3 patients, and twenty-five (69.5%) T4 patients. A total of 30 TDs and 55 MLNs were identified. Of the 36 patients with gastric cancer, 18 had TDs; 15 had less than 3 TDs, and 3 had 3 or more TDs. Table 1 shows the baseline characteristics of the patients with gastric cancer

Table 1
Baseline characteristics of the patients with gastric cancer.

	Patients with TDs only (n = 4)	Patients with MLNs only (n = 18)	Patients with both TDs and MLNs(n = 14)
Age(mean)	66.75	64.17	66.00
Sex(males/females)	3/1	13/5	10/4
CA-724median (P25, P75), U/mL	6.59(1.81,23.9)	4.31(1.40,32.96)	11.97(3.93,39.68)
CEA median (P25, P75), ng/mL	2.28(1.67,19.02)	2.59(2.15,12.80)	4.60(1.66,10.77)
Histologic grade			
Poorly differentiated	2	10	9
Moderately differentiated	2	7	5
Well differentiated	0	1	0
T status			
1/2	1	1	1
3	1	5	2
4	2	12	11
N status			
1	2	3	0
2	0	4	4
3	2	11	10
Perineural invasion (Absence/Presence)	1/3	11/7	2/12
Lymphovascular invasion (Absence/Presence)	0/4	2/16	0/14

ICC analysis

The ICCs of the parameters measured by the two radiologists ranged from 0.752 to 0.981, indicating high interrater reliability. The measurement parameters of the senior radiologist were statistically analyzed. The results of the consistency analysis of the imaging findings are presented in Table 2.

Table 2
Results of the consistency analysis of the imaging findings.

Imaging manifestations	ICC	95% CI
Irregular morphology	0.841	0.756–0.897
Necrosis	0.813	0.713–0.878
Long-axis diameter (mm)	0.981	0.971–0.988
Short-axis diameter (mm)	0.980	0.969–0.987
Aspect ratio (%)	0.752	0.619–0.839
cCAV in Noncontrast phase (%)	0.859	0.782–0.908
cCAV in Arterial phase (%)	0.903	0.851–0.937
cCAV in Venous phase (%)	0.906	0.855–0.939
cCAV in Delayed phase (%)	0.940	0.908–0.961

***:**ICC=intraclass correlation coefficient, cCAV= corrected CT attenuation value

Comparison of CT morphology and parameter measurements between the TD and MLN groups

In the TD group, most of the lesions were large (median long-axis diameter = 14.55 mm, median short-axis diameter = 12.16 mm). Of the 30 TDs, 15 were necrotic, and 21 had irregular morphology (Figs. 3–5). In the MLN group, most of the lesions were small (median long-axis diameter = 12.07 mm, median short-axis diameter = 10.11 mm). Of the 55 MLNs, 34 were isoattenuating, and 44 had regular morphology (Figs. 6–8). The long- and short-axis diameters of the lesions in the TD group were larger than those in the MLN group. The cCAV in each phase was higher in the TD group than in the MLN group, and the cCAV in each phase was significantly different between the TD and MLN groups ($P < 0.05$). There were no significant differences in necrosis or the aspect ratio (ratio of the long-axis diameter to the short-axis diameter) between the two groups ($P > 0.05$). Table 3 compares the CT morphology and parameter measurements between the TD group and the MLN group.

Table 3
Comparisons of CT morphology and measurements of multiple parameters in the TD group and the MLN group.

Parameters	TD group (n = 30)	MLN group (n = 55)	χ^2/Z	*P* value
Irregular morphology: negative	9(30.0)	44(80.0)		
positive	21(70.0)	11(20.0)	20.674	**0.000**
Negative necrosis: negative	15(50.0)	34(61.8)		
positive	15(50.0)	21(38.2)	1.110	0.292
Long-axis diameter (mm)	14.55(10.16)	12.07(5.36)	-2.800	**0.005**
Short-axis diameter (mm)	12.16(8.06)	10.11(4.99)	-3.163	**0.002**
Aspect ratio (%)	113.29(18.38)	115.57(23.60)	-0.405	0.686
cCAV in Noncontrast phase (%)	93.09(10.73)	85.11.(22.13)	-3.444	**0.001**
cCAV in Arterial phase (%)	13.13(7.19)	8.53(9.14)	-3.724	**0.000**
cCAV in Venous phase (%)	39.60(14.05)	29.03(17.53)	-3.803	**0.000**
cCAV in Delayed phase (%)	36.69(13.56)	30.10(14.96)	-4.032	**0.000**
*:Bold type indicates $P < 0.05$, which is statistically significant.				
CT = computed tomography, TD = tumor deposit, MLN = metastatic lymph node, cCAV = corrected CT attenuation value,				

Comparison of CT morphological manifestations and diagnostic value of multiparameter measurements

The irregular lesion morphology, long-axis diameter, short-axis diameter, and cCAV in each phase all had AUCs greater than 0.685 for the diagnosis of TDs. Among them, the cCAV in the delayed phase (AUC = 0.766) had the highest diagnostic efficacy. The optimal diagnostic threshold was 32.94%. The corresponding diagnostic sensitivity was 80.00%, and the specificity was 67.27%.

The ROC curve of irregular lesion morphology had a sensitivity of 70.00%, a specificity of 80.00%, and an AUC of 0.750 ($P = 0.000$). The ROC curve of a long-axis diameter of 16.65 mm had a sensitivity of 40.00%, a specificity of 92.73%, and an AUC of 0.679 ($P = 0.007$). The ROC curve of a short-axis diameter of 10.27 mm had a sensitivity of 83.33%, a specificity of 54.54%, and an AUC of 0.708 ($P = 0.001$). Similarly, the ROC curves of a cCAV in the noncontrast phase of 85.20%, a cCAV in the arterial phase of 10.64%, a cCAV in the venous phase of 33.99%, and a cCAV in the delayed phase of 32.94% had

sensitivities of 76.67–86.67%, specificities of 50.91–69.09%, and AUCs of 0.727–0.766 (all $P < 0.05$) (Table 4,Fig. 9).

Table 4
The diagnostic efficacy of each parameter for differentiating TDs from MLNs.

Parameters	AUC	Optimal cutoff point	Sensitivity	Specificity	*P* value	95% CI
Irregular morphology	0.750	-	70.00	80.00	**0.000**	0.636–0.864
Long-axis diameter (mm)	0.685	≥16.65	40.00	92.73	**0.005**	0.564–0.805
Short-axis diameter (mm)	0.708	≥10.27	83.33	54.54	**0.002**	0.593–0.824
cCAV in Noncontrast phase (%)	0.727	≥85.20	86.67	50.91	**0.001**	0.621–0.833
cCAV in Arterial phase (%)	0.745	≥10.64	76.67	69.09	**0.000**	0.641–0.850
cCAV in Venous phase (%)	0.751	≥33.99	76.67	67.27	**0.000**	0.649–0.852
cCAV in Delayed phase (%)	0.766	≥32.94	80.00	67.27	**0.000**	0.666–0.866

*****TDs = tumor deposits, MLNs = metastatic lymph nodes, AUC = area under the ROC curve,cCAV = corrected CT attenuation value

Discussion

Many studies [9, 14–16] have shown that TDs are an important prognostic factor for GC. According to Anup et al. [17], the prognoses of patients with TDs in the pT1–3 category were identical to those in the pT4a category, indicating that TDs may be better handled as a type of serosal invasion. As a result, en bloc resection of the primary tumor is critical, and adjuvant treatment should always be considered if TDs are found. In addition, Sun et al. [16] observed that the number of TDs was positively correlated with worsening prognosis. As the number of TDs increased, the five-year survival rate of patients decreased gradually. Many other studies [18, 19] have emphasized that TDs differ from MLNs because the former have a worse effect on prognosis. Therefore, accurate diagnosis of perigastric TDs and MLNs in gastric cancer before treatment is conducive to the selection of appropriate treatment regimens and the assessment of prognosis. Currently, there are four main types of imaging examinations for gastric cancer patients: MDCT, endoscopic ultrasonography (EUS), magnetic resonance imaging (MRI), and positron emission tomography (PET)/CT [20]. MDCT is widely used in gastric cancer patients due to its fast scanning speed, high spatial resolution, and stable image quality [21], but there are relatively few studies

on the use of MDCT to evaluate perigastric TDs in gastric cancer. We hope that the preoperative CT evaluation of perigastric TDs in gastric cancer can help doctors determine treatment strategies more accurately and select the best type of surgery for their patients.

In our study, we used contrast-enhanced CT to distinguish between perigastric TDs and MLNs in gastric cancer. The contrast-enhanced CT images of 36 patients with gastric cancer were analyzed, and the morphological characteristics and parameters of contrast-enhanced CT in the pathologically confirmed TDs (30) and MLNs (55) were evaluated. The results showed that morphology and size could be used to differentiate TDs from MLNs. Most TDs have irregular morphology, and some have lobulation and spiculation. This irregular morphology may be caused by the proliferation, migration, and accumulation of tumor cells and their heterogeneous growth in different directions, or it may be related to the formation of TDs. Puppa et al. [22] believed that TDs may be a new type of destructive metastatic invasion involving blood vessels and perivascular structures. Most MLNs have a smooth appearance and regular morphology (mostly round or oval). In terms of pathological manifestation, in MLNs, the tumor cells are encapsulated by the lymph nodes due to the immune response and are not able to grow beyond the lymph node capsule. Regular morphology is an important appearance factor that can be used to distinguish TDs from MLNs. However, it has been reported that MLNs can also have irregular morphology, perhaps because the tumor grows in the lymph nodes and gradually invades them [23].

In this study, the long-axis and short-axis diameters of TDs were larger than those of MLNs. It is possible that TDs contain more tumor cells than MLNs and grow faster. Atre et al. [24] showed that on MRI, TDs adjacent to rectal cancer have an irregular morphology and larger long- and short-axis diameters than MLNs, a finding that is consistent with the results of this study. In our study, the aspect ratios of TDs and MLNs were not significantly different, perhaps because TDs tend to be round or oval overall despite having an irregular morphology. In addition, the cCAVs in each phase were significantly higher in the TD group than in the MLN group, possibly due to the high density of tumor cells and the abundance of tumor blood vessels in TDs, characteristics that can also be used to differentiate between TDs and MLNs.

To date, research on perigastric TDs in gastric cancer has mainly focused on their prognostic value and how to reasonably include them in TNM staging [25, 26]. The present study is the first to predict TDs in gastric cancer by using CT imaging. With the continuous innovation and development of CT technology, the diagnostic information obtained using CT is no longer limited to morphological manifestations and CT values of lesions but also incorporates other functions. such as dual energy CT (DECT), CT-perfusion (CTp) and radiomics, etc. [27–31]. The application of these methods to MLNs in gastric cancer has been studied previously, but the prediction of gastric cancer TDs by these methods remains to be verified. In addition, in an imaging study of TDs in rectal cancer, Lord et al. [32] reported that TDs are related to nodules in the intramesorectal venous pathways on MRI images that mainly connect to the venous branches and do not connect to the primary tumor. This new prognostic marker is included in the MRI report and is called mrTDs. Lord et al. [32] also showed that mrTDs and extramural venous invasion (mrEVMI) on MRI images have higher prognostic accuracy than the current clinical TNM staging of rectal cancer. However, because gastric veins are more abundant, slender, and tortuous than rectal veins and

because contrast-enhanced CT has a poorer ability than MRI to display gastric veins, the conclusions of Lord et al. could not be verified in the present work. In future studies, we will combine dual DECT, CTp, MRI and radiomics to make more accurate judgments regarding perigastric TDs in gastric cancer, predict the disease condition of patients, and inform accurate and reasonable treatments for patients in clinical practice.

This study has the following limitations. (1) Because all of the nodules examined in this study had a diameter greater than 5 mm, nodules with diameters less than 5 mm may have been missed. Even when nodules have a diameter less than 2 mm, the possibility of TDs and MLNs cannot be excluded [33, 34]. (2) Some of the available data were lost because it was difficult to correspond some of the TDs or MLNs with CT images. The difficulty of one-to-one correspondence in surgery increases with decreasing nodule volume, resulting in a certain bias in the selection of nodules. In addition, the sample size was relatively small. The selected measurement parameters failed to show all of the imaging characteristics of TDs. In future studies, we will need to expand the sample size and enrich the measurement parameters to obtain more abundant and more accurate data. (3) No CT examinations performed using DECT, CTp, or radiomics are available for comparison with enhanced CT imaging in the evaluation or detection of TDs.

In conclusion, this study demonstrates that contrast-enhanced MDCT scanning is beneficial for predicting TDs in patients with gastric cancer prior to surgery. The lesion morphology and size observed by MDCT and the cCAVs in the noncontrast phase and each contrast-enhanced phase have reference value for differentiating between perigastric TDs and MLNs. TD-positive gastric cancer patients have poor prognosis. Hence, predicting and identifying TDs through preoperative contrast-enhanced CT can guide clinicians in selecting more suitable treatment regimens to maximize the benefits of treatment.

Abbreviations

MDCT=multidetector computed tomography, TDs=tumor deposits, MLN=metastatic lymph node, CT=computed tomography, ROC=receiver operating characteristic, CAV=CT attenuation value, cCAV= corrected CT attenuation value, AUC=area under the ROC curve, AJCC=American Joint Committee on Cancer, ROI=region of interest, PACS=picture archiving and communication system, WL=window level, WW=window width, ICC=intraclass correlation coefficient, EUS=endoscopic ultrasonography, MRI=magnetic resonance imaging, PET=positron emission tomography, DECT=dual-energy CT, CTp=CT-perfusion

Declarations

Acknowledgements

Not applicable

Authors' contributions

Conception and design: WZ; Administrative support: WZ; Provision of study materials or patients: all authors; Collection and assembly of data: HG,YW,CL; Data analysis and interpretation: all authors; Manuscript writing: HG; All authors reviewed the results and approved the final version of the manuscript.

Funding

This study is supported by Keynote Research of the Natural Science Foundation of Liaoning Province (2019JH8/10300035).

Availability of data and materials

The datasets used during the current study are available from the corresponding author on reasonable request.

Ethics approval and consent to participate

This study was approved by ethical committees of The First Affiliated Hospital of Jinzhou Medical University and informed consent to participate has been given by patients included into this trial.

Consent for publication

Not applicable

Competing interests

The authors declare that they have no competing interests.

Author details

1. Department of Radiology, The First Affiliated Hospital of Jinzhou Medical University

2. Department of Gastrointestinal surgery, The First Affiliated Hospital of Jinzhou Medical University

3. Department of Pathology Department, The First Affiliated Hospital of Jinzhou Medical University

References

1. Smyth EC, Nilsson M, Grabsch HI, van Grieken NC, Lordick F. Gastric cancer. Lancet (London, England)2020; 396 (10251):635-648.
2. Yang Y, Ma Y, Xiang X, Xing P, Wu Y, Zhang L, et al. The prognostic value of the lymph node ratio for local advanced gastric cancer patients with intensity-modulated radiation therapy and concurrent

chemotherapy after radical gastrectomy in China. Radiation oncology (London, England)2020; 15 (1):237.

3. Ren F, Li S, Zhang Y, Zhao Z, Wang H, Cui Y, et al. Efficacy and safety of intensity-modulated radiation therapy versus three-dimensional conformal radiation treatment for patients with gastric cancer: a systematic review and meta-analysis. Radiation oncology (London, England)2019; 14 (1):84.
4. Amin MB, Edge SB, Greene F, Wallner G. AJCC Cancer Staging Manual. eighth ed.New York: Springer; 2017.
5. Gabriel WB, Dukes C, Bussey H. Lymphatic spread in cancer of the rectum. Brit J Surg2010; 23 (90):395–413.
6. Puppa G, Ueno H, Kayahara M, Capelli P, Canzonieri V, Colombari R, et al. Tumor deposits are encountered in advanced colorectal cancer and other adenocarcinomas: an expanded classification with implications for colorectal cancer staging system including a unifying concept of in-transit metastases. Mod Pathol2009; 22 (3):410–415.
7. Graham Martínez C, Knijn N, Verheij M, Nagtegaal ID, van der Post RS. Tumour deposits are a significant prognostic factor in gastric cancer: a systematic review and meta-analysis. Histopathology2019; 74 (6):809–816.
8. Anup S, Lu J, Zheng CH, Li P, Xie JW, Wang JB, et al. Prognostic significance of perigastric tumor deposits in patients with primary gastric cancer. BMC Surg2017; 17 (1):84.
9. Gu L, Chen P, Su H, Li X, Zhu H, Wang X, et al. Clinical Significance of Tumor Deposits in Gastric Cancer: a Retrospective and Propensity Score-Matched Study at Two Institutions. J Gastrointest Surg2020; 24 (11):2482-2490.
10. Peparini N. Beyond T, N and M: The impact of tumor deposits on the staging and treatment of colorectal and gastric carcinoma. Surg Oncol2018; 27 (2):129-137.
11. Wenquan L, Yuhua L, Jianxin C, Hongqing X, Kecheng Z, Jiyang L, et al. Tumor deposit serves as a prognostic marker in gastric cancer: A propensity score-matched analysis comparing survival outcomes. Cancer Med2020; 9 (10):3268-3277.
12. Wang X, Ye H, Yan Y, Wu J, Wang N, Chen M. The Preoperative Enhanced Degree of Contrast-enhanced CT Images: A Potential Independent Predictor in Gastric Adenocarcinoma Patients After Radical Gastrectomy. Cancer Manag Res2020; 12:11989-11999.
13. Wang Y, Liu W, Yu Y, Han W, Liu JJ, Xue HD, et al. Potential value of CT radiomics in the distinction of intestinal-type gastric adenocarcinomas. European radiology2020; 30 (5):2934-2944.
14. Liang Y, Wu L, Liu L, Ding X, Wang X, Liu H, et al. Impact of extranodal tumor deposits on prognosis and N stage in gastric cancer. Surgery2019; 166 (3):305-313.
15. Graham Martínez C, Knijn N, Verheij M, Nagtegaal ID, van der Post RS. Tumour deposits are a significant prognostic factor in gastric cancer - a systematic review and meta-analysis. Histopathology2019; 74 (6):809-816.
16. Sun Z, Wang Z-n, Xu Y-y, Zhu G-l, Huang B-j, Xu Y, et al. Prognostic significance of tumor deposits in gastric cancer patients who underwent radical surgery. Surgery2012; 151 (6):871-881.

17. Anup S, Lu J, Zheng C-H, Li P, Xie J-W, Wang J-B, et al. Prognostic significance of perigastric tumor deposits in patients with primary gastric cancer. BMC Surg2017; 17 (1):84.
18. Tonouchi A, Sugano M, Tokunaga M, Sugita S, Watanabe M, Sato R, et al. Extra-perigastric Extranodal Metastasis is a Significant Prognostic Factor in Node-Positive Gastric Cancer. World J Surg2019; 43 (10):2499-2505.
19. Tan J, Yang B, Xu Z, Zhou S, Chen Z, Huang J, et al. Tumor deposit indicates worse prognosis than metastatic lymph node in gastric cancer: a propensity score matching study. Ann Transl Med2019; 7 (22):671.
20. Giganti F, Orsenigo E, Arcidiacono PG, Nicoletti R, Albarello L, Ambrosi A, et al. Preoperative locoregional staging of gastric cancer: is there a place for magnetic resonance imaging? Prospective comparison with EUS and multidetector computed tomography. Gastric Cancer2016; 19 (1):216–225.
21. Jeong O, Jung M, Kang J, Ryu S. Prognostic performance of preoperative staging: assessed by using multidetector computed tomography-between the new clinical classification and the pathological classification in the eighth American joint committee on cancer classification for gastric carcinoma. Ann Surg Oncol2020; 27 (2):545–551.
22. Puppa G, Maisonneuve P, Sonzogni A, Masullo M, Capelli P, Chilosi M, et al. Pathological assessment of pericolonic tumor deposits in advanced colonic carcinoma: relevance to prognosis and tumor staging. Mod Pathol2007; 20 (8):843–855.
23. Li B, Wong IY, Chan FS, Chan KK, Wong CL, Law T, et al. Impact of extracapsular extension of lymph node in adenocarcinoma of the stomach. Ann Surg Oncol2020; 27 (11):4225–4232.
24. Atre ID, Eurboonyanun K, Noda Y, Parakh A, O'Shea A, Lahoud RM, et al. Utility of texture analysis on T2-weighted MR for differentiating tumor deposits from mesorectal nodes in rectal cancer patients, in a retrospective cohort. Abdom Radiol (NY)2021; 46 (2):459–468.
25. Peparini N. Beyond T, N and M: The impact of tumor deposits on the staging and treatment of colorectal and gastric carcinoma. Surgical oncology2018; 27 (2):129-137.
26. Anup S, Lu J, Zheng CH, Li P, Xie JW, Wang JB, et al. Prognostic significance of perigastric tumor deposits in patients with primary gastric cancer. BMC Surg2017; 17 (1):84.
27. Li J, Dong D, Fang M, Wang R, Tian J, Li H, et al. Dual-energy CT-based deep learning radiomics can improve lymph node metastasis risk prediction for gastric cancer. European radiology2020; 30 (4):2324-2333.
28. Sun Z, Li J, Wang T, Xie Z, Jin L, Hu S. Predicting perigastric lymph node metastasis in gastric cancer with CT perfusion imaging: A prospective analysis. Eur J Radiol2020; 122:108753.
29. Dong D, Fang MJ, Tang L, Shan XH, Gao JB, Giganti F, et al. Deep learning radiomic nomogram can predict the number of lymph node metastasis in locally advanced gastric cancer: an international multicenter study. Annals of oncology : official journal of the European Society for Medical Oncology2020; 31 (7):912-920.

30. Song BI. Nomogram using F-18 fluorodeoxyglucose positron emission tomography/computed tomography for preoperative prediction of lymph node metastasis in gastric cancer. World journal of gastrointestinal oncology2020; 12 (4):447-456.
31. Jin Y, Li M, Zhao Y, Huang C, Liu S, Liu S, et al. Computed Tomography-Based Radiomics for Preoperative Prediction of Tumor Deposits in Rectal Cancer. Frontiers in oncology2021; 11:710248.
32. Lord AC, D'Souza N, Shaw A, Rokan Z, Moran B, Abulafi M, et al. MRI-diagnosed tumour deposits and emvi status have superior prognostic accuracy to current clinical TNM staging in rectal cancer. Ann Surg2020.
33. Nagtegaal ID, Knijn N, Hugen N, Marshall HC, Sugihara K, Tot T, et al. Tumor Deposits in Colorectal Cancer: Improving the Value of Modern Staging-A Systematic Review and Meta-Analysis. J Clin Oncol2017; 35 (10):1119-1127.
34. Fukuya T, Honda H, Hayashi T, Kaneko K, Tateshi Y, Ro T, et al. Lymph-node metastases: efficacy for detection with helical CT in patients with gastric cancer. Radiology1995; 197 (3):705-711.

Figures

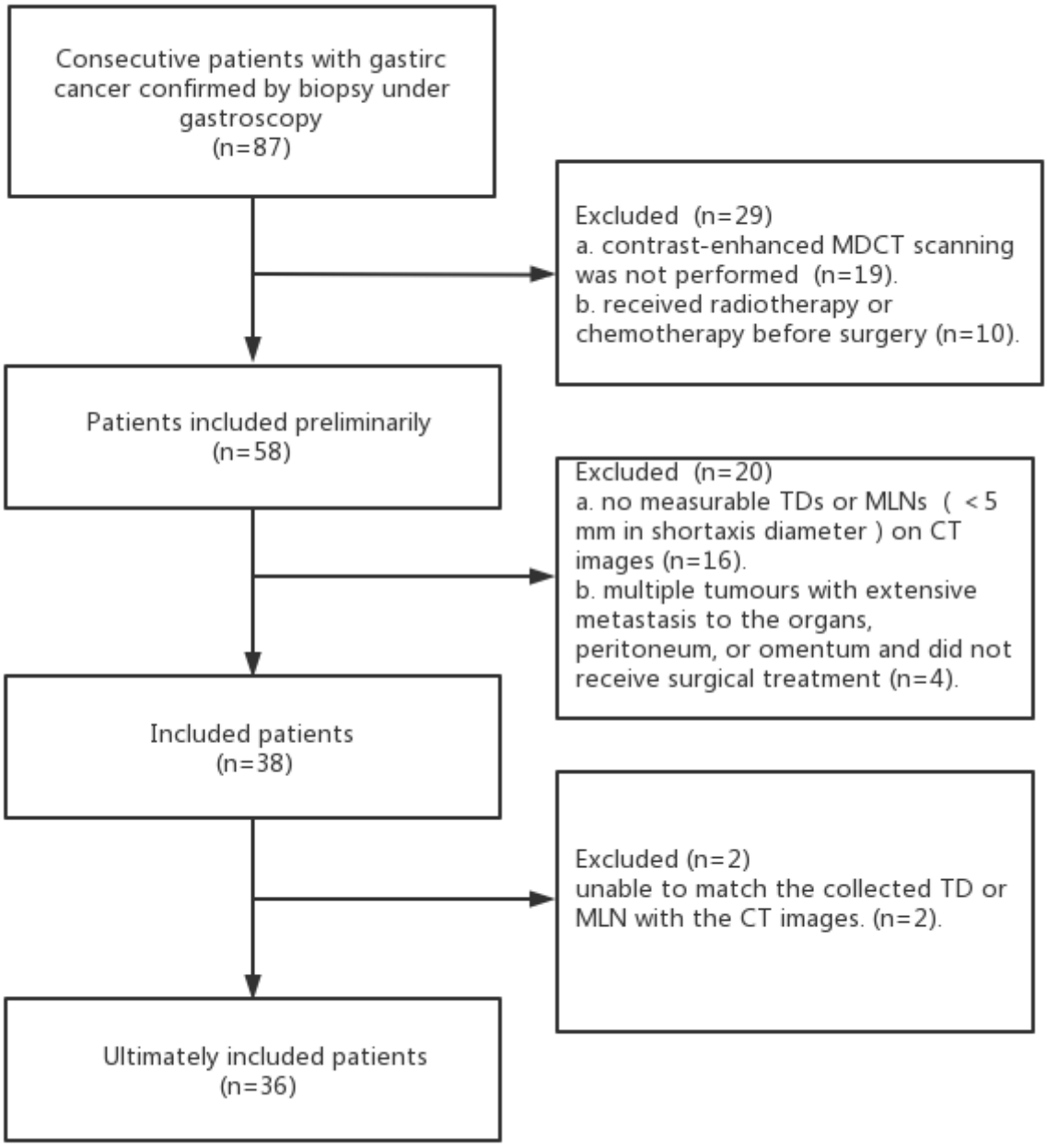

Figure 1

Flowchart of patient selection.

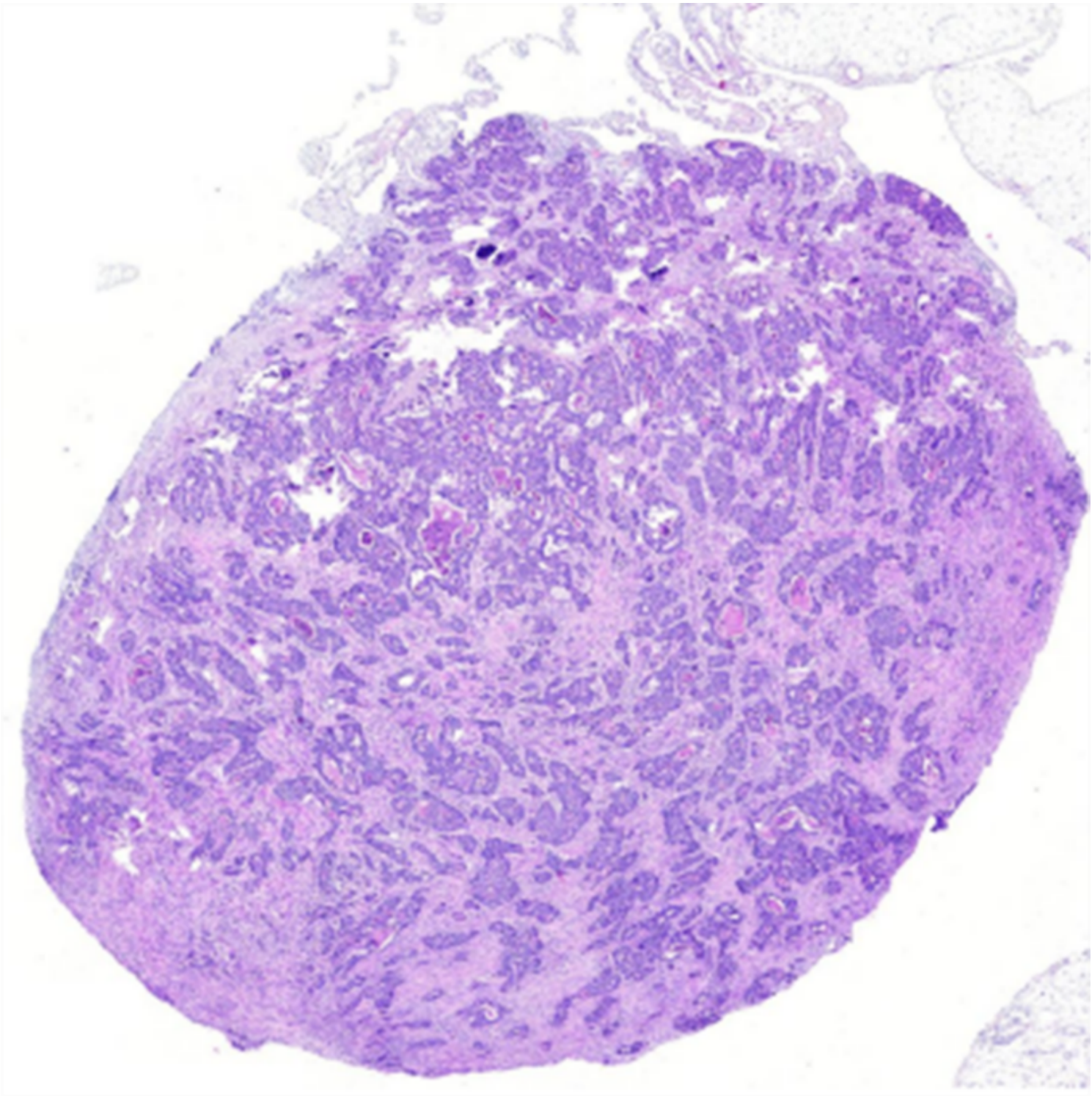

Figure 2

Pathological HE staining of TDs in gastric cancer (×1).

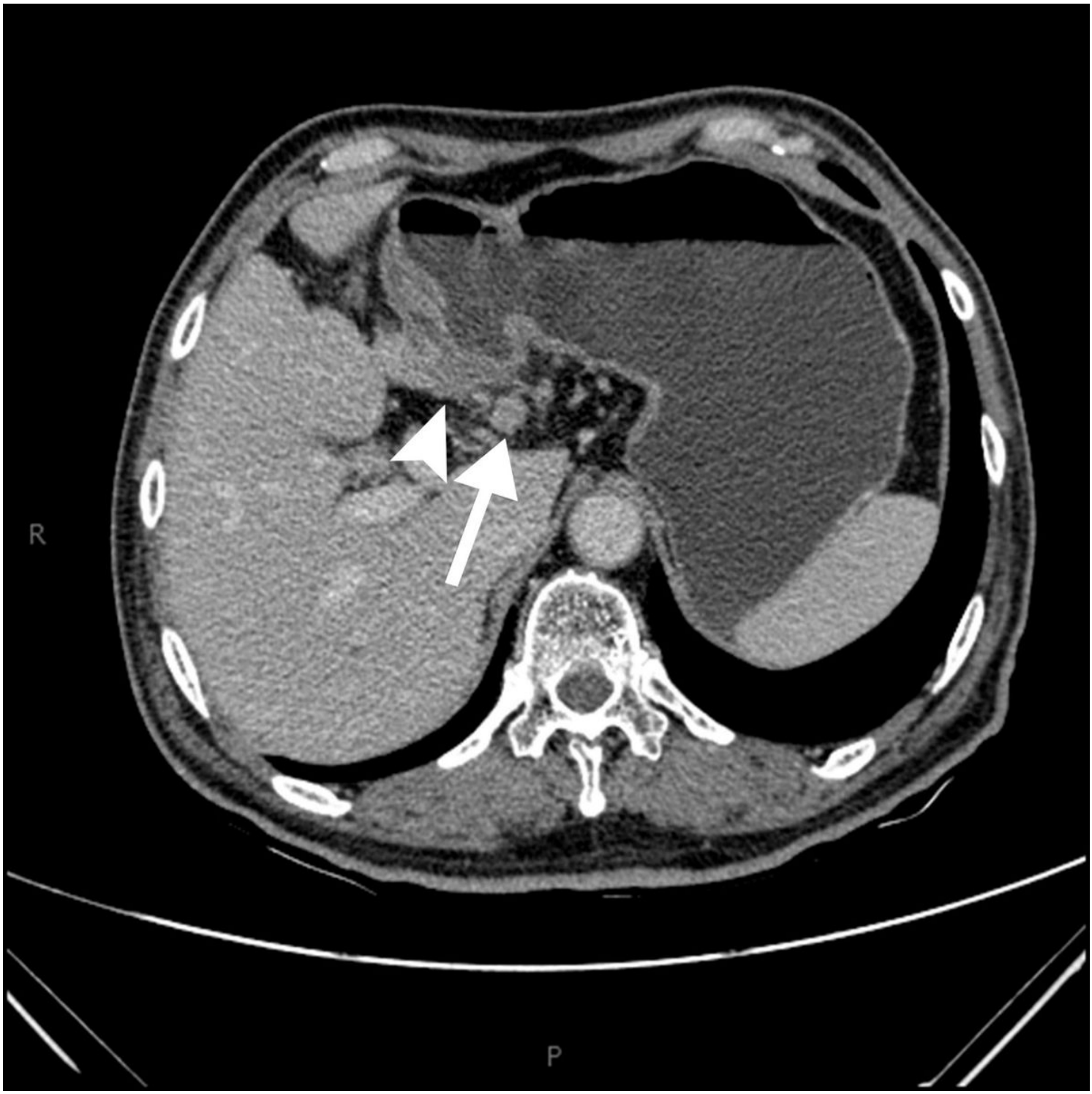

Figure 3

Perigastric TDs in a 60-year-old male patient with gastric cancer. The axial contrast-enhanced CT image of the entire abdomen showed that the gastric wall was thickened in the gastric antrum (arrow) and that the TDs had irregular morphology, lobulation and spiculation (long arrows).

Figure 4

Perigastric TDs in a 70-year-old male patient with gastric cancer. The reconstructed coronal contrast-enhanced CT image of the entire abdomen showed that the TDs had irregular morphology and lobulation (long arrow).

Figure 5

Perigastric TDs in a 66-year-old female patient with gastric cancer. The axial contrast-enhanced CT image of the entire abdomen showed that the gastric wall was thickened and enhanced in the gastric antrum (arrow) and that the TDs had lobulation and unenhanced necrotic areas in the center (long arrow).

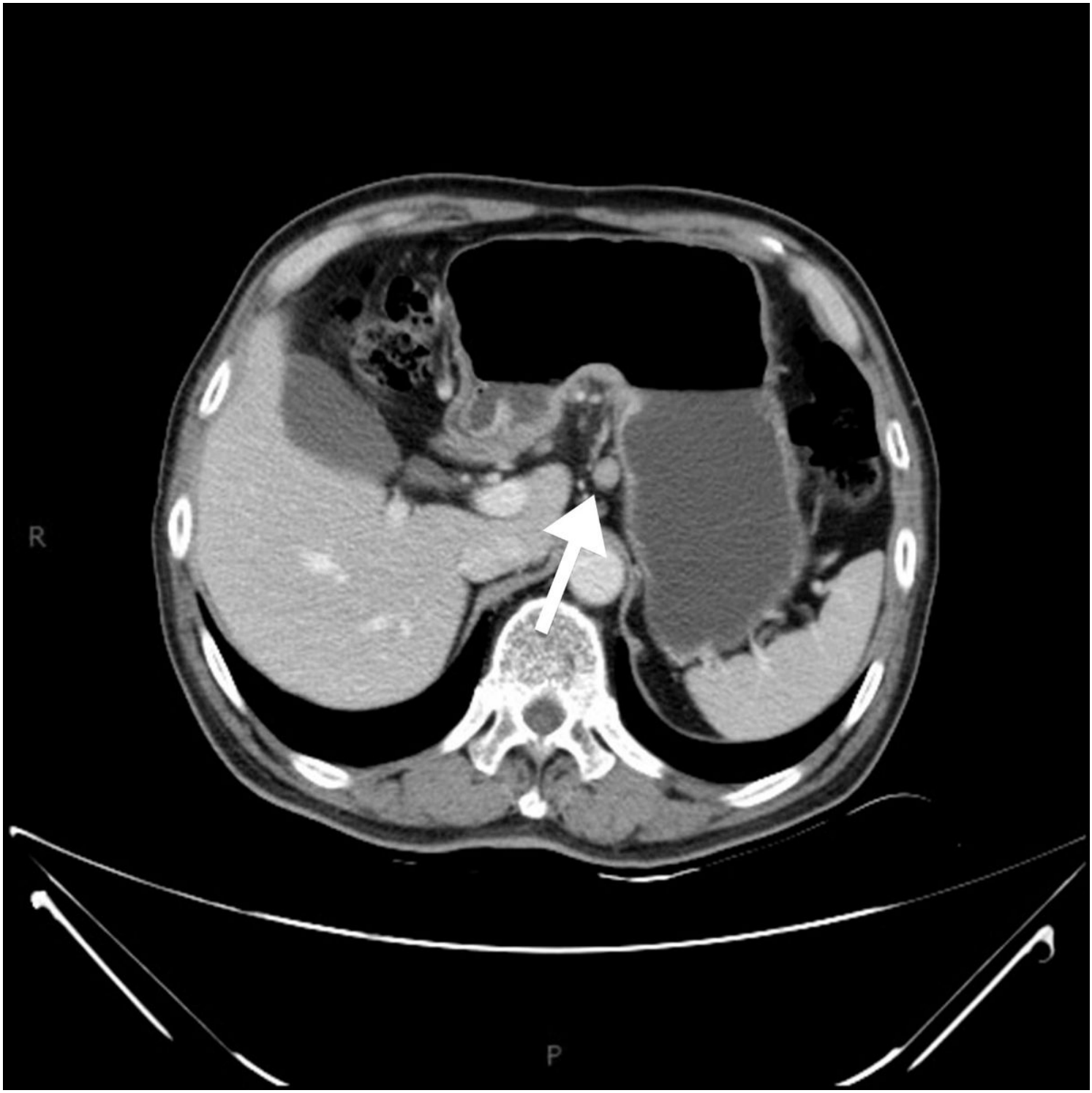

Figure 6

Perigastric MLNs in a 64-year-old male patient. The axial contrast-enhanced CT image of the entire abdomen showed that the MLNs in the lesser curvature had regular shapes and well-defined margins (long arrow).

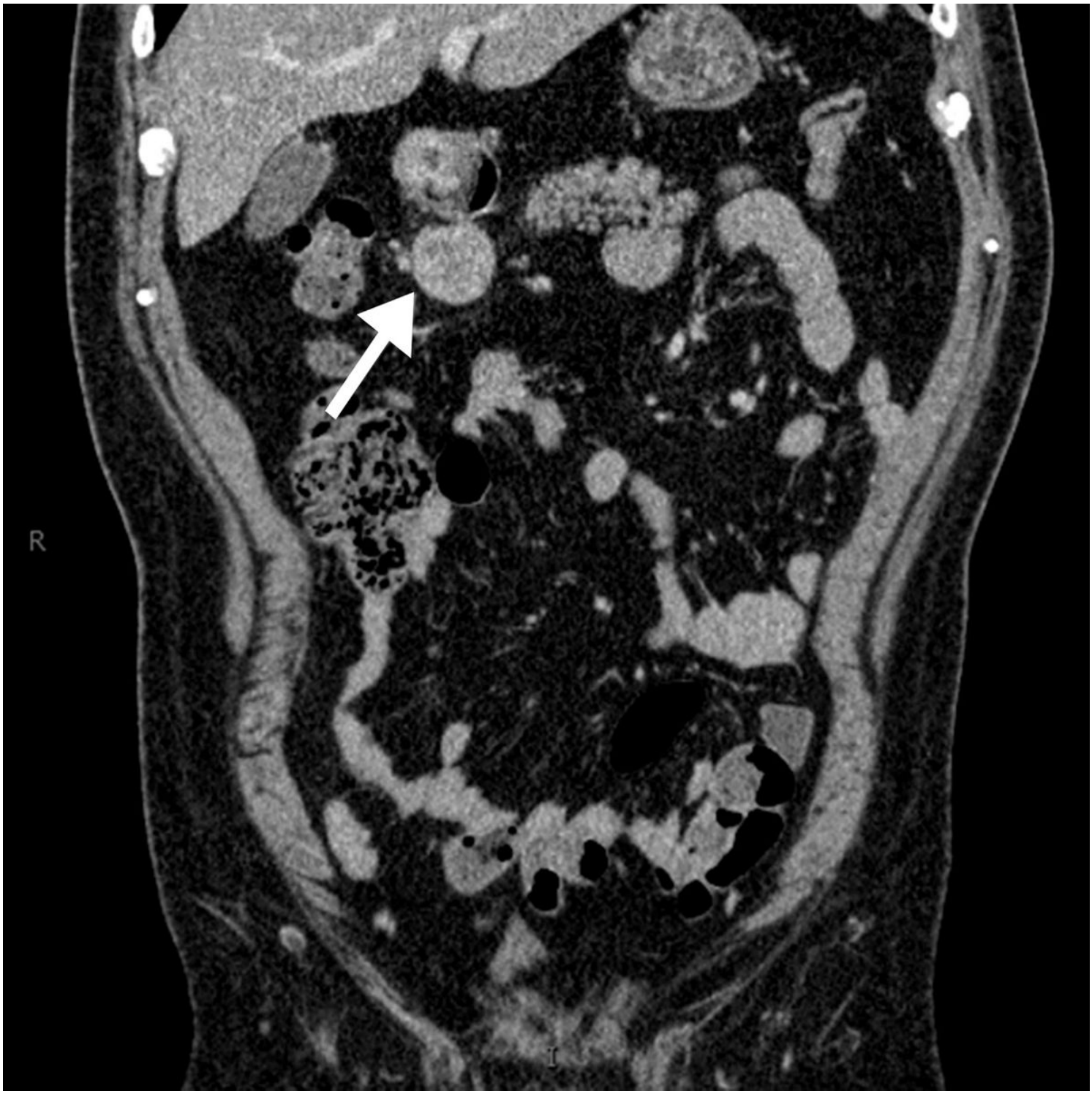

Figure 7

Perigastric MLNs in a 64-year-old male patient. The reconstructed coronal CT-enhanced image of the entire abdomen showed that the MLNs in the lesser curvature had regular shapes and homogeneous enhancement (long arrow).

Figure 8

Perigastric MLNs in a 62-year-old male patient. The axial contrast-enhanced CT image of the entire abdomen showed that the gastric wall had heterogeneous thickening in the lesser curvature (arrow) and that the MLNs in the lesser curvature had regular shapes, well-defined margins, and unenhanced necrotic areas in the center.

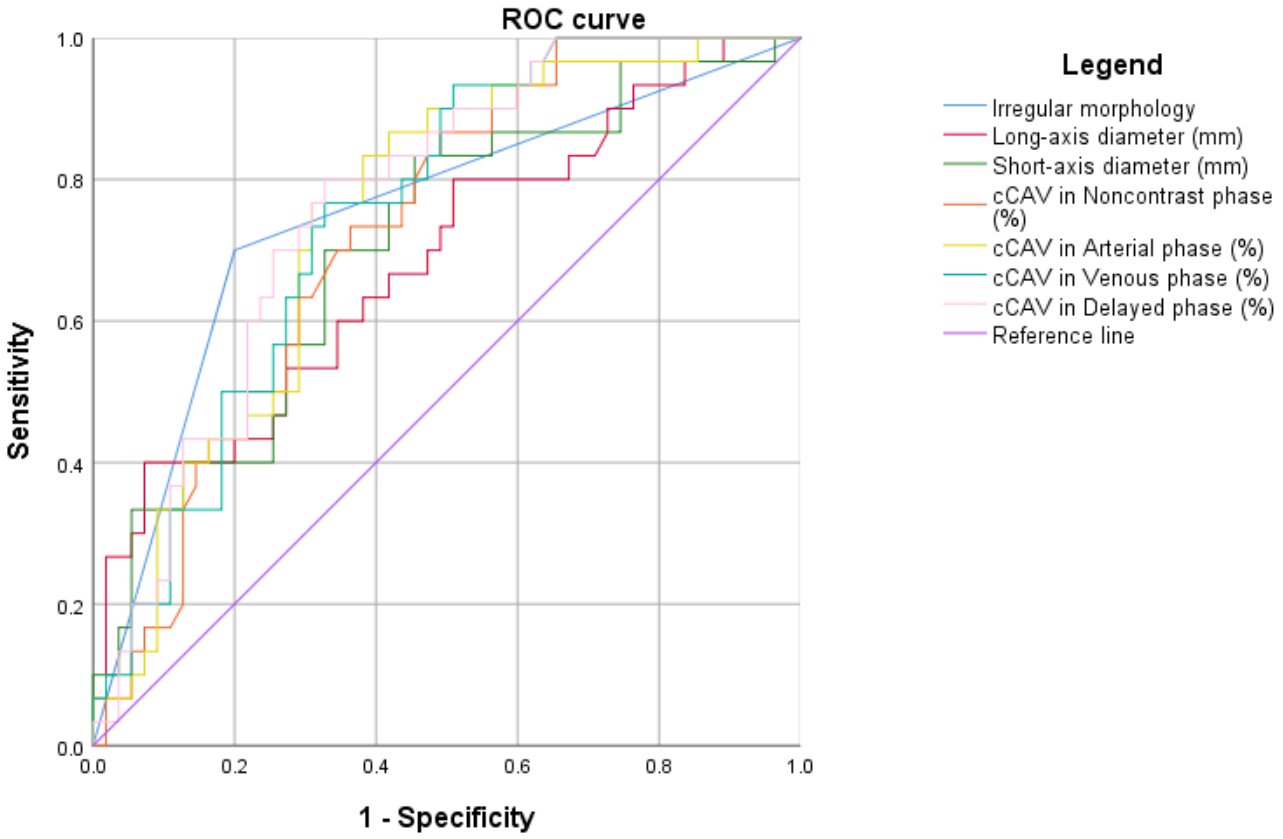

Figure 9

A graph showing the ROC curve for the diagnostic efficacy of each parameter for differentiating TDs from MLNs.

*: TDs=tumor deposits, CT=computed tomography, MLN=metastatic lymph node, ROC=receiver operating characteristic